THE ROYAL SOCIETY

Received 21 August 2003
Accepted 4 November 2003

Evidence for an elastic projection mechanism in the chameleon tongue

Jurriaan H. de Groot[1] **and Johan L. van Leeuwen**[2*]

[1] *Section of Evolutionary Morphology, Institute of Biology, Leiden University, PO Box 9516, 2300 RA Leiden, The Netherlands*
[2] *Experimental Zoology Group, Wageningen Institute of Animal Sciences, Wageningen University, Marijkeweg 40, 6709 PG Wageningen, The Netherlands*

To capture prey, chameleons ballistically project their tongues as far as 1.5 body lengths with accelerations of up to 500 m s^{-2}. At the core of a chameleon's tongue is a cylindrical tongue skeleton surrounded by the accelerator muscle. Previously, the cylindrical accelerator muscle was assumed to power tongue projection directly during the actual fast projection of the tongue. However, high-speed recordings of *Chamaeleo melleri* and *C. pardalis* reveal that peak powers of 3000 W kg^{-1} are necessary to generate the observed accelerations, which exceed the accelerator muscle's capacity by at least five- to 10-fold. Extrinsic structures might power projection via the tongue skeleton. High-speed fluoroscopy suggests that they contribute less than 10% of the required peak instantaneous power. Thus, the projection power must be generated predominantly within the tongue, and an energy-storage-and-release mechanism must be at work. The key structure in the projection mechanism is probably a cylindrical connective-tissue layer, which surrounds the entoglossal process and was previously suggested to act as lubricating tissue. This tissue layer comprises at least 10 sheaths that envelop the entoglossal process. The outer portion connects anteriorly to the accelerator muscle and the inner portion to the retractor structures. The sheaths contain helical arrays of collagen fibres. Prior to projection, the sheaths are *longitudinally* loaded by the combined radial contraction and hydrostatic lengthening of the accelerator muscle, at an estimated mean power of 144 W kg^{-1} in *C. melleri*. Tongue projection is triggered as the accelerator muscle and the loaded portions of the sheaths start to slide over the tip of the entoglossal process. The springs relax *radially* while pushing off the rounded tip of the entoglossal process, making the elastic energy stored in the helical fibres available for a simultaneous forward acceleration of the tongue pad, accelerator muscle and retractor structures. The energy release continues as the multilayered spring slides over the tip of the smooth and lubricated entoglossal process. This sliding-spring theory predicts that the sheaths deliver most of the instantaneous power required for tongue projection. The release power of the sliding tubular springs exceeds the work rate of the accelerator muscle by at least a factor of 10 because the elastic-energy release occurs much faster than the loading process. Thus, we have identified a unique catapult mechanism that is very different from standard engineering designs. Our morphological and kinematic observations, as well as the available literature data, are consistent with the proposed mechanism of tongue projection, although experimental tests of the sheath strain and the lubrication of the entoglossal process are currently beyond our technical scope.

Keywords: chameleon; tongue; projection mechanism; catapult; elastic energy; power output

1. INTRODUCTION

Prey capture in the chameleon occurs over four different phases. First, prey distance is estimated (Harkness 1977; Ott & Schaeffel 1995) and the tongue slowly protrudes between the jaws (phase I; see also figure 1*a–c*). Second, the tongue accelerates forward (phase II; Bell 1990; Wainwright *et al.* 1991; Wainwright & Bennett 1992*a*; Herrel *et al.* 2000), at up to 490 m s^{-2} (*Chamaeleo oustaleti*; Wainwright *et al.* 1991). Third, after a period of near constant velocity (phase III), the tongue pad decelerates (phase IV; see also figure 1*a,c*) and the prey is caught by active prehension (Herrel *et al.* 2000) and adhesion to the tongue pad. Finally, the retractor muscle withdraws the tongue back into the mouth (Rice 1973; Wainwright & Bennett 1992*a*,*b*).

The first hypotheses about tongue projection (reviewed by Gnanamuthu 1930; Zoond 1933) invoked tongue erection by inflowing blood or inflating of the tongue from the lungs. Duvernoy (1836) first proposed a specialized muscular system that projects the tongue, and many studies assumed the accelerator muscle to be the direct effector of tongue projection (e.g. Zoond 1933; Gnanamuthu 1937; Altevogt & Altevogt 1954; Gans 1967; Bell 1990; Wainwright *et al.* 1991; Wainwright & Bennett 1992*a*,*b*; Van Leeuwen 1997). Zoond (1933) established the currently held view that the accelerator muscle exerts a normal stress on the tapering tip of the entoglossus. The forward-directed reaction force on the tongue pad projects the tongue off the entoglossal process. The cylindrical muscle slides over the tip of the entoglossal process and contracts, reducing its inner diameter. A negative pressure gradient along the active accelerator muscle might contribute to the forward motion (Van Leeuwen 1997). This mechanism requires that the accelerator muscle can generate enough power to accelerate the tongue.

By contrast, Van Leeuwen *et al.* (2000) proposed that the accelerator muscle could power tongue projection indirectly by storing elastic energy in connective tissues,

---

[*] Author for correspondence (johan.vanleeuwen@wur.nl).

DOI 10.1098/rspb.2003.2637

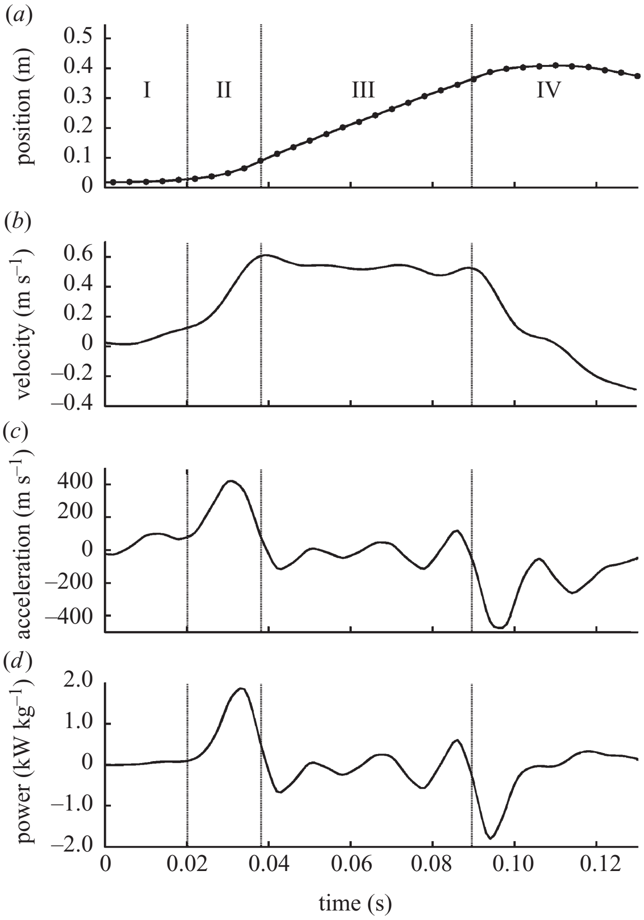

Figure 1. (*a*) Position, (*b*) velocity, (*c*) acceleration and (*d*) the derived mass-specific power output for the tongue motion in *Chamaeleo melleri* while catching a locust, obtained from video recordings (250 frames s^{-1}) by digitizing tongue position (black dots in (*a*)). Four phases are indicated: I, protrusion; II, acceleration (projection phase); III, ballistic flight; IV, deceleration.

which is later released to accelerate the tongue forward. A thick layer of connective tissue between the entoglossal process and the accelerator muscle connects the tip of the entoglossal process with the inner fascia of the accelerator muscle (Gnanamuthu 1930; Zoond 1933; Gans 1967; Herrel *et al.* 2001*a*). This was thought to play a regulating and/or lubricating role during projection. Gnanamuthu (1930) recognized several layers of 'tendons' around the entoglossal process. Bell (1989) described inner and outer layers of connective tissue.

The aims of this paper are threefold. To test whether the accelerator muscle can power tongue projection, we use kinematic analysis. We investigate a possible intrinsic elastic storage-and-release mechanism in the tongue by studying the morphology of the hyobranchial apparatus and the soft tissues within the tongue. Finally, we investigated to what extent extrinsic structures (muscle and connective tissue) might transmit power to tongue pad via the entoglossal process as suggested by Wainwright *et al.* (1991). We quantified the contributions of the intrinsic and extrinsic structures to tongue projection using high-speed X-ray video images of *in vivo* prey-capture events (Snelderwaard *et al.* 2002).

2. MORPHOLOGICAL OBSERVATIONS

Two specimens of *C. pardalis*, one specimen of *C. jacksonii* and two specimens of *C. chamaeleon* were used for morphological dissections of the hyolingual complex. The fibre types in the connective tissue that envelops the entoglossal process were determined by applying Van Gieson staining (for collagen) and Weigert's resorcin–fuchsin staining (for elastin).

We focus on structures that may be involved directly in tongue projection, i.e. the entoglossal process, a part of the tongue skeleton, and the soft tissues mounted on the entoglossal process. Extrinsic tongue muscles, such as the genioglossus muscle, can transmit power to the projected tongue mass only via the entoglossal process. Four important structural elements were identified in the studied tongues.

(i) The core of the tongue is the entoglossal process (figures 2*b*, 3 and 4*a*), a cylindrical parallel-sided cartilage surrounded by a thick and smooth layer of thick longitudinal collagen fibres, the perichondrium. The entoglossal process tapers only in its distal 1–1.5%, if at all (Herrel *et al.* 2001*a*; cf. figure 3*a*). Wainwright & Bennett (1992*b*) mention a slight taper of the anterior 9% of the entoglossal process in *C. jacksonii*. Its tip is rounded and thickened dorsally by connective tissue (figure 3; indicated as 'articulating cartilagenous tip' by Herrel *et al.* (2001*a*)), which connects to the inner surface of the covering connective tissue (figures 2*c* and 3). The often visible longitudinal taper of the entoglossal process (figure 2*b*; e.g. Gans 1967) results from sections that deviate (both in position and orientation) from the mid-sagittal plane.

(ii) The paired hyoglossi or retractor muscles (see figures 2*b* and 4*a*) envelop the posterior portion of the entoglossal process and connect anteriorly to the lateral surface of the accelerator muscle (Rice 1973; Bell 1989; Herrel *et al.* 2001*b*). The retractor muscles attach internally to a cylindrical epimysial fascia (figure 4). The muscular part and the internal fascia are here referred to as the retractor complex. In the resting position, the inactive retractor muscles are pleated, and the pitch angle of the collagen fibres in the internal epimysium is *ca.* 85° (figure 4*b*(i)).

(iii) The cylindrical accelerator muscle envelops a thick layer of connective tissue (see item iv). The muscle fibres are arranged in transverse planes and form clockwise and anticlockwise spiral-shaped arcs that extend from the peripheral boundary to the internal boundary (Gnanamuthu 1937; Bell 1989; Van Leeuwen 1997; figure 4*a*(ii)). Muscle tissue is almost incompressible (Wainwright & Bennett 1992*b*; Van Leeuwen 1997). Hence, when the muscle contracts along the entoglossal process, it becomes thinner and elongates at the same time. The inner and outer surfaces of the muscle are covered by epimysial layers of connective tissue with helically arranged collagen fibres.

(iv) The thick layer of connective tissue between the entoglossal process and the accelerator muscle (figures 2*b* and 4*a*) connects the flexible and 'articulating' tip of the entoglossal process with the inner fascia of the accelerator muscle (Gnanamuthu 1930;

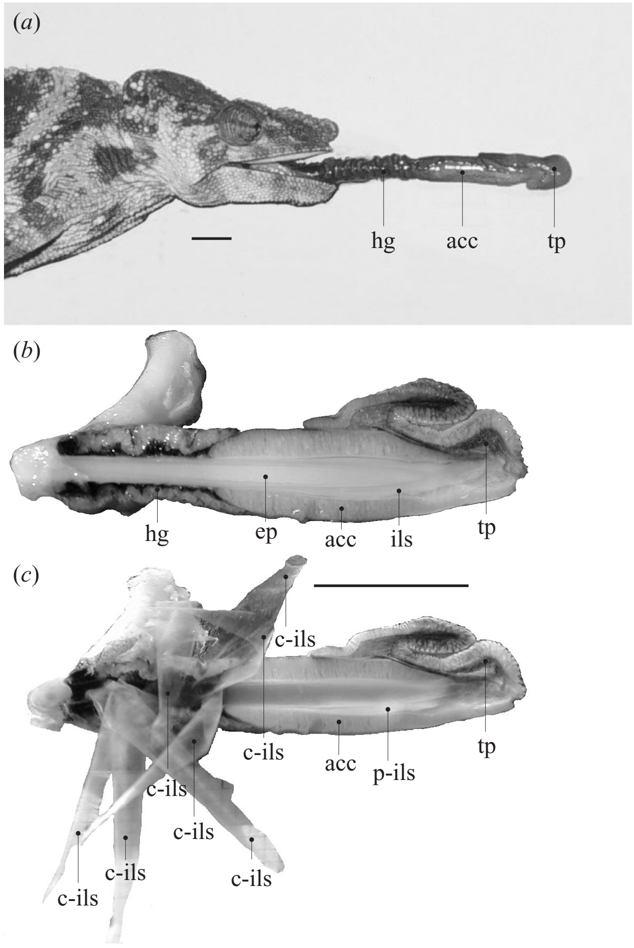

Figure 2. (*a*) Lateral view of *Chamaeleo melleri* during the acceleration phase of prey capture. The tongue pad (tp), the accelerator muscle (acc) and the retractor complex (hg) are simultaneously accelerated. (*b*) A close to sagittal section of the tongue of *Chamaeleo jacksonii*. The intralingual sheaths (ils) are mounted on the entoglossal process (ep), enclosed by the tubular structure formed by the accelerator muscle (acc) and the retractor complex (hg). The round entoglossal tip appears tapered owing to sectioning oblique to the mid-sagittal plane. (*c*) Same as (*b*), but now the entoglossal process is removed and the (sectioned) central sheaths (c-ils) are folded back to illustrate the nested structure of the intralingual collagen sheaths. The peripheral sheaths (p-ils) are still *in situ*, connected with the accelerator muscle. Scale bars, 10 mm.

Zoond 1933; Gans 1967; Bell 1989; Herrel *et al.* 2001*a*). However, a single tubular tendon connecting the fascia of the accelerator muscle and the tip of the entoglossal process cannot account for the observed tongue elongation during projection. Removing the entoglossal process from the sagitally sectioned tongue (figure 2*b*,*c*) revealed that the intralingual 'tendon' comprises a nested series of individual sheaths. The innermost sheath was attached to the posterior end of the fascia of the retractor muscle, near the articulation of the entoglossal process and the ceratobranchials. Each subsequent sheath connected slightly anterior to the preceding sheath. After removing this inner set of approximately nine nested sheaths (it is very hard to judge the exact number of thin sheaths from dissections or histological sections), a major portion of the 'tendon' was still present. The outer or peripheral tendon sheaths formed a thick layer, connected to the fascia of the accelerator muscle. At least six peripheral sheaths are mutually interconnected by collagenous trabeculae. The fibrous proteins in the nested intralingual sheaths contain collagen (Van Gieson staining), but no elastin (Weigert's resorcin–fuchsin staining). Collagen-fibre angles were measured on flattened and stained (picro-red) longitudinal sections (figure 4*b*). The inner cylindrical fascia of the accelerator muscle and the interconnected peripheral sheaths form a complex elastic unit. During tongue projection and elongation, the peripheral sheaths remain structurally associated with the tongue pad. The collagen fibres in the peripheral sheaths form clockwise and anticlockwise helices. The central sheaths are longer than the peripheral sheaths, and the caudally open ends of the central tubular sheaths are attached to the tubular and highly extendable retractor complex (figures 2*c* and 4*a*) at approximately evenly distributed intervals. The more central the location of the sheath, the greater its length and the further posterior its attachment point. The retractor complex is the only structural connection between the internal sheaths.

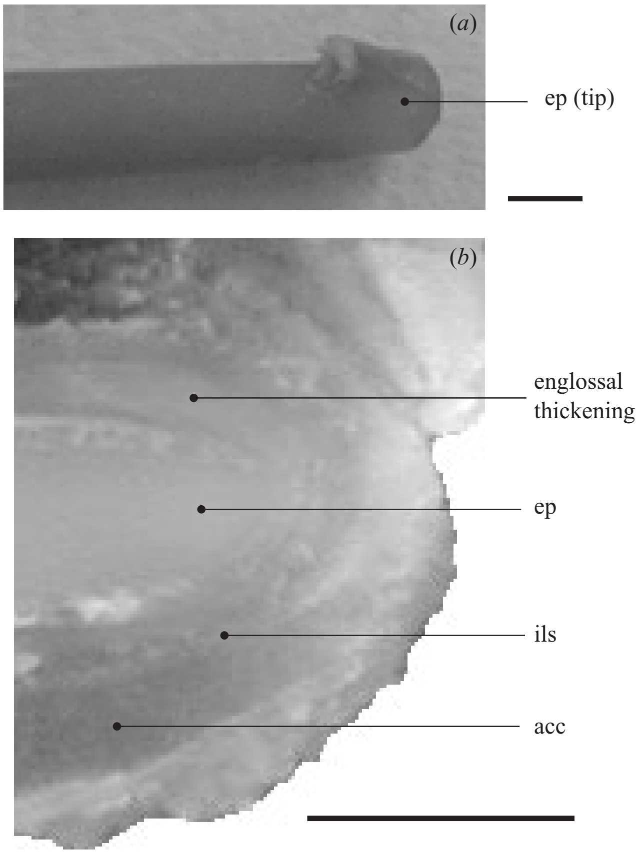

Figure 3. Details of the tip of the entoglossal process (ep) showing the dorsal thickening. (*a*) Lateral view of the entoglossal process of *Chamaeleo jacksonii*. Muscle tissue and intralingual sheaths were removed. (*b*) Close to mid-sagittal section of *C. jacksonii*. The entoglossal tip is thickened by connective tissue, i.e. the 'articulating cartilagenous tip' (Herrel *et al.* 2001*a*), which connects the perichondrium of the entoglossal process with the innermost intralingual collagen sheath. Abbreviations as in figure 2. Scale bars, 2 mm.

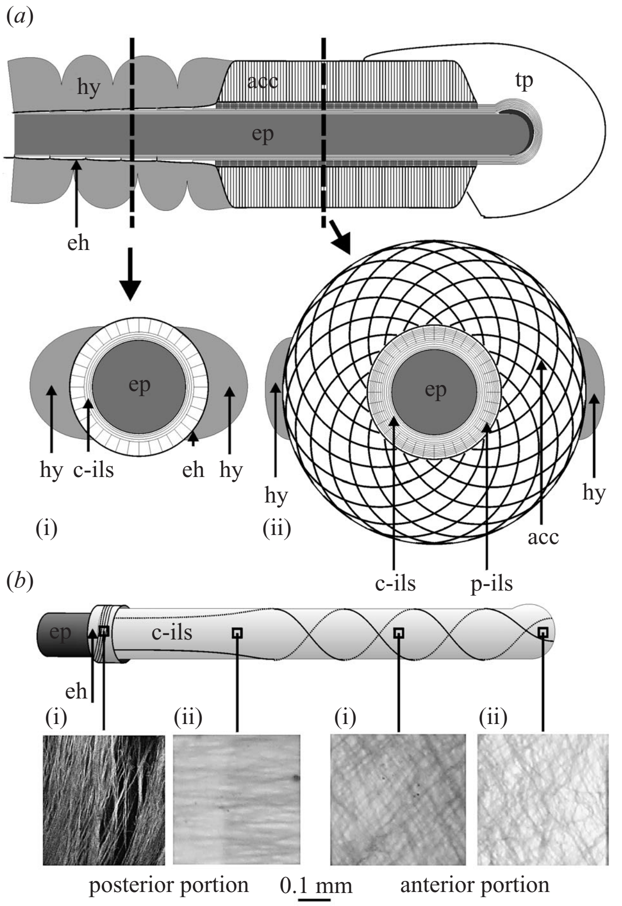

Figure 4. Drawings of the structures involved in the chameleon's tongue-projection mechanism: acc, accelerator muscle; hy, hyoglossus muscle, internally bound by a firm tubular epimysium (eh); c-ils, central intralingual sheaths; p-ils, peripheral intralingual sheaths; ep, entoglossal process; tp, tongue pad. (*a*) Mid-sagittal cross-section of the tongue. The entoglossal process (thickened at the tip) is enveloped by the intralingual sheaths. Proximally, the central intralingual sheaths connect to the tubular epimysium of the retractor complex; the more proximal the insertion, the longer the sheath. The maximum length of the peripheral lingual sheaths is determined by the proximal margin of the accelerator muscle; the sheaths interconnect mutually by crossing collagen fibres, and locally contain higher contents of glycoproteins (PAS positive). The peripheral lingual sheaths connect to the internal epimysium of the accelerator muscle. The central intralingual sheaths envelop the entoglossal process (i,ii). The posterior margins of the internal sheaths connect to the perimysium of the hyoglossus muscle at evenly distributed sites (i). Anteriorly, the central and peripheral intralingual sheaths envelop the entoglossal process (ii). The peripheral intralingual sheaths are mutually interconnected and connected to the fascia of the accelerator muscle. (*b*) Collagen-fibre orientations along the sheaths. (i) The retractor epimysium, fibre angle of *ca.* 85° to the longitudinal tongue axis; (ii) proximal sheath section, fibre angle *ca.* 6°; (iii) anterior section, fibre angle *ca.* 50°; (iv) tip section, fibrous network, with large variety of fibre directions.

There are no collagenous trabeculae between the sheaths, and the central sheaths are not attached to the accelerator muscle. The anterior portions of the central sheaths, which at rest are enveloped by the accelerator muscle, contain helical collagen fibres (figure 4*b*). The collagen fibres in the portions that are proximal to the accelerator muscle run parallel to the long axis of the entoglossal process (figure 4*b*(ii)). Thus, a nested series of tubular connective-tissue sleeves is mounted on the distal portion of the entoglossal process. The central nested sheaths are interconnected only by the retractor complex and can, in principle, slide along one another like the tubes of an extending telescope. Unlike a single tubular tendon connecting the entoglossal process with the fascia of the accelerator muscle, this structural arrangement conforms with the observed elongation of the projected tongue. The fibre arrangement in the anterior portion of the sheaths is consistent with nested elastic springs that can store and release energy.

Our morphological observations suggest three potential contributions to the acceleration of the soft tongue mass: (i) forward acceleration of the entoglossal process by extrinsic structures; (ii) the direct contribution of the accelerator muscle; and (iii) the quick release of elastic energy stored in the collagen fibres of the intralingual collagen sheaths and possibly also the epimysium of the accelerator muscle. Only the accelerator muscle could load elastic energy into these structures. To distinguish these three potential contributions, we recorded the motion of radio-opaque markers in the lingual complex with high-speed X-ray video and analysed their kinematics.

3. EXPERIMENTAL METHODS

The kinematics of the hyolingual complex was derived from high-speed videos (250 frames s^{-1}) of a specimen of *C. pardalis* (snout–vent length of 0.18 m; $n = 13$ recordings) and a specimen of *C. melleri* (snout–vent length of 0.23 m; $n = 25$ recordings). Coordinates of video images of landmarks on the specimens were digitized and low-pass filtered (recursive third-order Butterworth, cut-off frequency of 60 Hz). The velocity and acceleration of the landmarks during tongue protrusion were obtained by differentiation and double differentiation, respectively, of the filtered displacement data.

The same specimen of *C. melleri* was anaesthetized (O_2: $0.35\ \mathrm{l\ min}^{-1}$; N_2O with 2% isofluothane: $0.45\ \mathrm{l\ min}^{-1}$) and lead markers were fixed into the skeleton and onto the soft tissues of the tongue. After recovery, high-speed X-ray recordings were made at 500 frames s^{-1} and a shutter speed of 1/3000 s (Snelderwaard *et al.* 2002). The images were scaled and corrected for image distortions using a grid that was recorded in the plane of tongue projection, immediately after prey capture. The X-ray time traces of position coordinates were low-pass filtered (recursive third-order Butterworth) with a cut-off frequency of 65 Hz. All experiments were authorized by the local ethical committee on animal experiments (U-DEC98022).

The lead markers that were inserted halfway into the entoglossal process (marker 3 in figure 5*a*) allowed us to quantify the displacement of the tongue skeleton during the slow protrusion phase and the subsequent tongue projection.

Two markers were glued onto the posterior end of the accelerator muscle (markers acc in figure 5*a*). The position of these markers relative to the tip of the tongue (marker 1 in figure 5*a*) indicates the elongation of the accelerator muscle during the slow protrusion phase (suggested to occur by Wainwright & Bennett (1992*a*,*b*)). The marker displacement provides the velocity

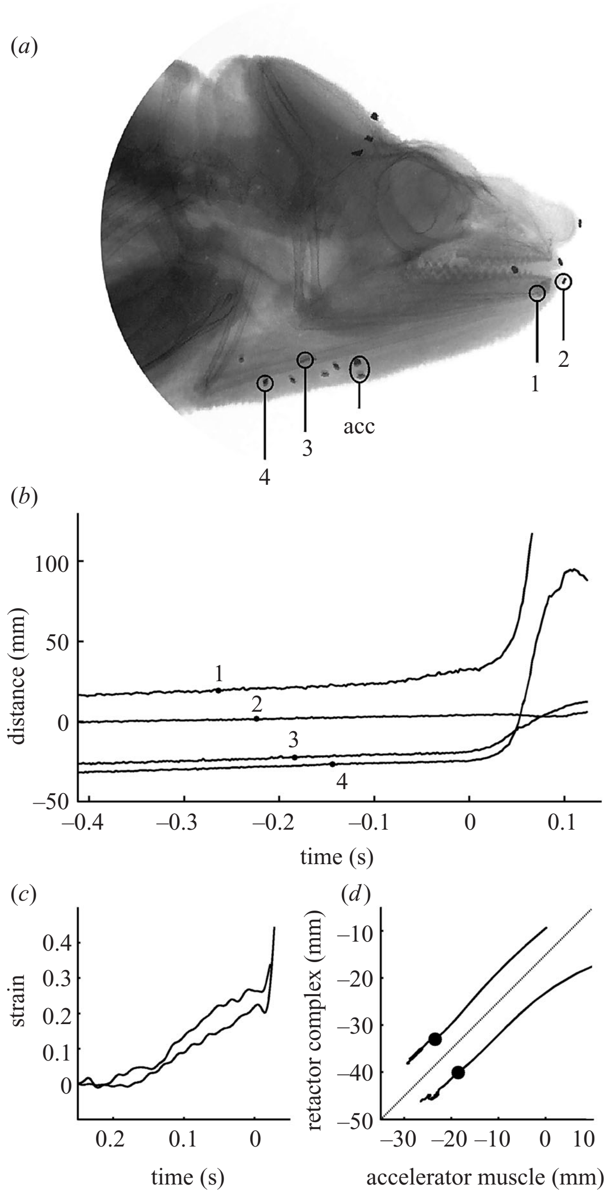

Figure 5. (*a*) Position and definition of radio-opaque markers: 1, tip of the tongue; 2, lower jaw; 3, in the entoglossal process; 4, glued to the retractor complex; acc, glued to the posterior end of the accelerator muscle. (*b*) High-speed X-ray (500 frames s^{-1}) position–time traces of radio-opaque markers of *Chamaeleo melleri* tongue while catching a locust. Digitized marker positions were all low-pass filtered (see § 3). Position of markers indicated in the X-ray photograph (*a*). (*c*) The longitudinal strain of the soft tissue between marker acc of the accelerator muscle and the tongue tip (marker 1) during the slow protrusion phase (phase I, figure 1), prior to tongue projection, which starts at $t = 0$ s. Two curves are shown for separate feeding events. A longitudinal strain occurs *ca.* 0.2 s prior to projection. The accelerator muscle covers only *ca.* 75% of the recorded distance. The maximum longitudinal strain of the accelerator muscle is therefore expected to be 33%. (*d*) The synchronized displacement of the markers on the retractor complex and the proximal border of the accelerator muscle. Results are shown for two recorded feeding scenes and different marker positions. Time runs from the lower left to the upper right along the curves. The start of tongue projection ($t = 0$) is indicated with a dot on the curves for both feeding events. The displacements of the marker acc relative to a marker on the retractor complex (i.e. marker 4) are parallel with the reference line, indicating synchronous and equal displacement. Different markers on the retractor muscle were used for the two feeding acts, which explains the different locations of the curves.

and acceleration of the posterior end of the muscle, both in an earth-bound frame of reference and relative to the entoglossal process. Insertion of markers at the anterior margin of the accelerator muscle would affect the projection of the tongue and was therefore avoided.

Four evenly distributed markers were glued onto the retractor complex (figure 5*a*; the most caudal 'retractor marker' is numbered 4). Initially, the connection between the inactive retractor complex (Wainwright & Bennett 1992*a*) and the accelerator muscle is slack and pleated. Internally, the retractor complex is connected to the central subset of intralingual sheaths. Consequently, if these intralingual sheaths are to contribute to the acceleration of the tongue, then the retractor complex must accelerate simultaneously with the accelerator muscle. The central sheaths pull forward at their attachment sites along the retractor if they are under tension. Alternatively, if the sheaths do not contribute to the forward acceleration, then the various portions of the retractor muscle will start to accelerate sequentially from anterior to posterior, each portion accelerating only after the initial slack between the accelerator muscle and the retractor mass has vanished and their connection comes under tension. The progressive *forward acceleration* of the retractor complex would significantly *decelerate* the tongue tip during ballistic flight (figure 1; phase III). Our results show that this is not the case (§ 4c).

Markers were also fixed onto the anterior tip of the lower jaw (marker 2 in figure 5*a*), onto the skull and onto the cerato-branchial cartilage, but these were not used for the analysis presented here.

4. RESULTS AND DISCUSSION

(a) *Video analysis falsifies the accelerator muscle as the main direct effector of tongue projection*

Figure 1 shows the displacement, velocity and acceleration of the tongue tip during a typical feeding event of *C. melleri*. The calculated specific tongue power peaks at *ca.* 1800 W kg^{-1}. From high-speed video observations of *C. pardalis* and *C. melleri*, we calculated average maximum accelerations of the tongue pad of 340 m s^{-2} (s.d. = 33 ms^{-2}) and 374 m s^{-2} (s.d. = 25 ms^{-2}), respectively, of the tongue pad. The mechanical power output per unit mass of the tongue pad was calculated as the product of instantaneous velocity and acceleration. The average maximum mass-specific power output at the tongue pad was 1170 W kg^{-1} (s.d. = 176 W kg^{-1}) for *C. pardalis* and 1584 W kg^{-1} (s.d. = 176 W kg^{-1}) for *C. melleri*. The accelerator muscle accounts for *ca.* 50% of the mass of the tongue pad (in fact slightly more in *C. melleri*). Assuming a direct muscular power mechanism, the accelerator muscle must produce a maximum mass-specific power output of *ca.* 2340 W kg^{-1} (*C. pardalis*) or 3168 W kg^{-1} (*C. melleri*). These values are more than five times higher than the maximum mass-specific power outputs reported for most fast muscles. For example, the isolated sartorius muscle of *Rana pipiens* generates 371 W kg^{-1} at 25 °C (Lutz & Rome 1994), one of the highest recordings for vertebrate muscles. Recently, a power output of *ca.* 800 W kg^{-1} has been reported for the pectoralis muscle of the blue-breasted quail (Askew & Marsh 2001).

In conclusion, the present analysis falsifies the hypothesis that the accelerator muscle is the main direct power source of tongue projection. Two possible candidates remain: (i) an external source that conveys its power to the tongue pad via the entoglossal process; and (ii) the nested collagen sheaths that envelop the entoglossal process. In the latter case, the accelerator muscle might still be the prime energy source for projection if it stores elastic energy in the sheaths prior to projection and the sheaths release this energy at a faster rate during projection.

(b) *The accelerator muscle is active and elongates prior to projection*

The motion of several radio-opaque markers was tracked during tongue projection for a limited range of motion, confined within the boundaries of the X-ray field (figure 5*a*). The time traces of the tongue tip (marker 1), the jaw (marker 2), the entoglossal process (marker 3) and the retractor complex (marker 4), illustrate our findings (figure 5*b*). Prey was positioned *ca.* 25–30 cm from the chameleon, but the projection distance could not be measured exactly because the prey was necessarily outside the field of view.

During the phase of slow tongue protraction ($t = -0.2$ s until $t = 0$ s), the tongue skeleton protruded and the accelerator muscle started to deform 200 ms prior to projection (figure 5*c*). In this phase, the distance between the tip of the tongue and the marker glued to the posterior end of the accelerator muscle increased by 25% for the most extreme elongation recorded (figure 5*c*). The accelerator muscle, which is mainly responsible for elongation, covers only *ca.* 75% of the measured distance, hence it must have elongated by *ca.* 33%. The peak velocity of the tongue was 5 m s^{-1}. We now know that the accelerator muscle elongates during the slow phase of tongue protraction, a finding confirmed by the *in situ* observations of Zoond (1933). Wainwright & Bennett (1992*a*) demonstrated the onset of electrical activity in the accelerator muscle *ca.* 200 ms prior to tongue projection as well as a muscular elongation of up to 47% during artificial activation *in vitro*. From these observations, we conclude that the accelerator muscle is active during its elongation and is thus likely to generate mechanical work prior to tongue projection. The crucial role of the accelerator muscle in tongue projection is confirmed by observations that artificial stimulation of this muscle led to tongue projection (Zoond 1933), and that tongue projection was impossible after denervation of this muscle (Meyers & Nishikawa 2000).

Could the accelerator muscle produce all the required work (calculated from a peak kinetic energy of 72 mJ for our studied specimen of *C. melleri*, with a tongue mass of 4 g (mainly accelerator muscle and tongue pad) and a maximum velocity of 6 m s^{-1} for the recorded peak performance) in the active period before projection (*ca.* 200 ms)? The mass of the accelerator muscle is *ca.* 2 g. This would require a mean specific power output of *ca.* 180 W kg^{-1} prior to projection, which is well within the physiological range for fast twitch muscle fibres.

The only structures that could change their energetic state as a result of work produced by the accelerator muscle are the adjacent epimysial coverings of the muscle and the intralingual sheaths.

(c) *Contribution of the intralingual sheaths*

The intralingual sheaths fall into two groups based on their structure. The short peripheral sheaths are interconnected and fixed to the epimysium of the accelerator muscle. These sheaths may act as a parallel elastic unit of the accelerator muscle. However, the present experiments cannot determine the contributions of individual sheaths, because introducing radio-opaque markers sufficiently large to be detected by the X-ray equipment would have interfered with the proper functioning of the tongue system.

The longer and more central sheaths do not have interconnections and insert on the fascia of the retractor complex. The markers on the retractor complex therefore indicate the positions of the posterior ends of the longer intralingual sheaths.

During tongue projection, the markers on the retractor complex and the accelerator muscle (figure 5*d*) move almost simultaneously. The different portions of the retractor complex that are inactive during projection (Wainwright & Bennett 1992*a*), and have a slack connection to the accelerator muscle, were nevertheless accelerated simultaneously with the accelerator muscle. Within the tongue apparatus, only the intralingual sheets are in a position to generate the accelerating forces on the entire retractor complex because each sheath connects with its posterior end to this complex. These connections correspond to the lengths of the different sheaths, distributed over the entire length of the folded retractor complex and lend strong support to the aforementioned force-transmitting role in the projection process. The simultaneous forward acceleration of both tongue pad and retractor complex results in a ballistic flight with a more or less constant forward velocity. As mentioned in § 3, sequential forward acceleration of the retractor complex would decelerate the tongue tip during ballistic flight. Instead, we observed a constant-velocity plateau in feeding events over longer distances (e.g. figure 1).

If the sheaths pull the retractor complex forward, what accelerates the sheaths? The required forces are probably the reaction forces of the entoglossal process, which arise from the normal stress exerted by the sheaths under tension as they slide over the tip of the entoglossal process. Finally, full extension of the retractor complex is possible when the portions of the anterior sheath with helical fibres have slipped off the entoglossal complex, enabling the inner sheaths to slide along each other in a telescopic manner.

(d) *Power transmission via the entoglossal process*

In the projection phase, the entoglossal process moves forward, although very little compared with the displacements of the tongue tip and retractor complex (figure 5*b*). The contribution of the tongue skeleton and the soft tissues mounted onto the tongue skeleton was estimated from the time derivatives of their position data by the following calculations (figure 6). Let the stiff entoglossal process move forward with velocity v_{ent}. Assume that the soft tissue of the tongue can be represented by a single mass m_{tongue} that has velocity v_{tongue} and acceleration a_{tongue}. Let the tongue mass be connected to the entoglossal process

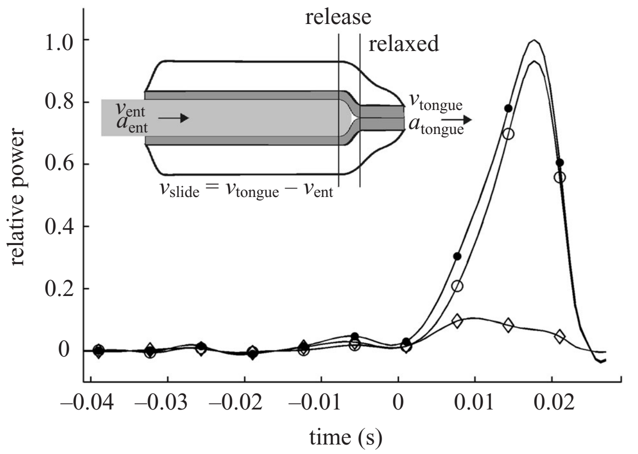

Figure 6. Relative power contributions of the entoglossal process (open diamonds) and the soft tissues mounted on it (open circles) to the total instantaneous power to the tongue pad (filled circles). Power values were normalized relative to the peak total power. Peak power transmission by the entoglossal process occurs before the power peak of the total system. More than 90% of the total power peak is generated by the soft tissues in the tongue. The contribution of the soft tissues is further explained in § 4d. The inset shows the central entoglossal process, the intralingual sheaths (dark grey, with a loaded region, a release zone and a relaxed portion) and the tongue pad (white), with the velocities and accelerations that were used to compute the respective powers as explained in § 4d. Calculations are based on digitized marker positions that were low-pass filtered with a cut-off frequency of 65 Hz (recursive third-order Butterworth).

via a tubular spring (representing the collection of tubular sheaths) that slides along the entoglossal process with a relative speed $v_{\mathrm{slide}} = v_{\mathrm{tongue}} - v_{\mathrm{ent}}$. The total power, P_{tot}, delivered to the tongue is $m_{\mathrm{tongue}}\ a_{\mathrm{tongue}}\ v_{\mathrm{tongue}}$. According to our sliding-spring theory, the spring contributes $P_{\mathrm{s}} = m_{\mathrm{tongue}}\ a_{\mathrm{tongue}}\ v_{\mathrm{slide}}$ to this total power, and the hyobranchial apparatus conveys via the entoglossal process an amount of $P_{\mathrm{ent}} = m_{\mathrm{tongue}}\ a_{\mathrm{tongue}}\ v_{\mathrm{ent}}$. The power contributions can be normalized relative to peak tongue power as: $P^*_{\mathrm{s}} = a_{\mathrm{tongue}}\ v_{\mathrm{slide}}/(a_{\mathrm{tongue}}\ v_{\mathrm{tongue}})_{\max}$ and $P^*_{\mathrm{ent}} = a_{\mathrm{tongue}}\ v_{\mathrm{ent}}/(a_{\mathrm{tongue}}\ v_{\mathrm{tongue}})_{\max}$ (figure 6; see table 1 in electronic appendix A). It appears that the peak power transmitted by the entoglossal process is *ca.* 10% of the total peak power. The efficacy of the power transmission by the entoglossal process depends on sufficient stiffness of the tongue pad. Peak power transmissions by the entoglossal process fall *ca.* 8 ms before the peak power of the total system, when most of the accelerator muscle and sheaths are still under considerable tension and thereby contributing to the stiffness of the tongue pad. The soft tissues mounted on the entoglossal process generate more than 90% of the peak power of the total system. Interestingly, the power contribution of the soft tissue is asymmetrical: the ascending slope is less steep than the descending slope. According to our theory and experimental findings, the strained portion of the spring slides with an increasing velocity along the entoglossal tip. Hence, the release rate of the locally stored energy per unit length should also increase (ascending slope of power curve), until the initially loaded spring extends completely beyond the entoglossal tip. After the peak, power should fall back very rapidly (the descending slope), but not instantaneously since the posterior 20% of the accelerator muscle tapers (figure 2) and therefore less energy per unit length is stored towards the posterior end. The steepness of the descending slope (and hence the asymmetry) may probably be underestimated in the experiment because we were forced to apply a low-pass filter (65 Hz cut-off frequency) owing to the limited accuracy of the X-ray movies.

Throughout the projection process, the tongue skeleton transmits *ca.* 15% of the work (i.e. the time integral of power represented by the surface under the power curve) for tongue projection. Consequently, *ca.* 85% of the total work must originate from the soft tissues mounted on the entoglossal process. Considering the recorded peak power performance of 3000 W kg^{-1} and assuming a maximum power output of muscular tissue of 400 W kg^{-1} (which presumably is an overestimate), at most 13% of the peak projection power could be generated instantaneously by the accelerator muscle and 10% was transmitted by the entoglossal process. The remaining 77% must stem from elastic tissues, pre-loaded by the work of the accelerator muscle prior to tongue projection. The contribution of the elastic component is presumably closer to 80–90%, because of the overestimated muscular power, which would require the accelerator muscle to generate *ca.* 144 W kg^{-1} over a period of 200 ms prior to projection for the peak performance of 6 m s^{-1}.

5. GENERAL DISCUSSION

We expect the proposed mechanism to be generally applicable to chameleons although the analysis was based on only a few species. We will therefore speak about 'the chameleon' in this discussion. Of course, details will vary among species. Considering (i) the physiological limitations of power production by muscular tissue, (ii) the low power contribution of the lingual skeleton to the tongue projection and (iii) the structural arguments for the acceleration of the retractor complex, an elastic release mechanism must be at work during the projection of the chameleon tongue. Three characteristics of the elastic mechanism are the muscular work prior to tongue projection, the elastic storage capacity of the generated work and a quick-release mechanism.

(a) *Muscular work prior to the tongue projection*

The accelerator muscle is active, elongates and is therefore likely to produce work prior to tongue projection, thereby loading the elastic intralingual collagen sheaths during the distributed forward motion of this muscle. The posterior margin of the accelerator muscle remains more or less in place, as is apparent from the radiographs. The accelerator muscle could deliver work on the sheaths by exerting normal stresses (at right angles to the outer sheath surface). These stresses cause longitudinal deformation according to the hydrostatic principle, generate longitudinal stresses in the collagen trabeculae that interconnect the peripheral sheaths and the accelerator muscle, and cause friction stresses (parallel to the outer sheath surface) and shear deformation as illustrated in figure 7. We made rough estimates of the longitudinal strain rate and the work that could be delivered by the radial and longitudinal muscular-force components, taking into account the

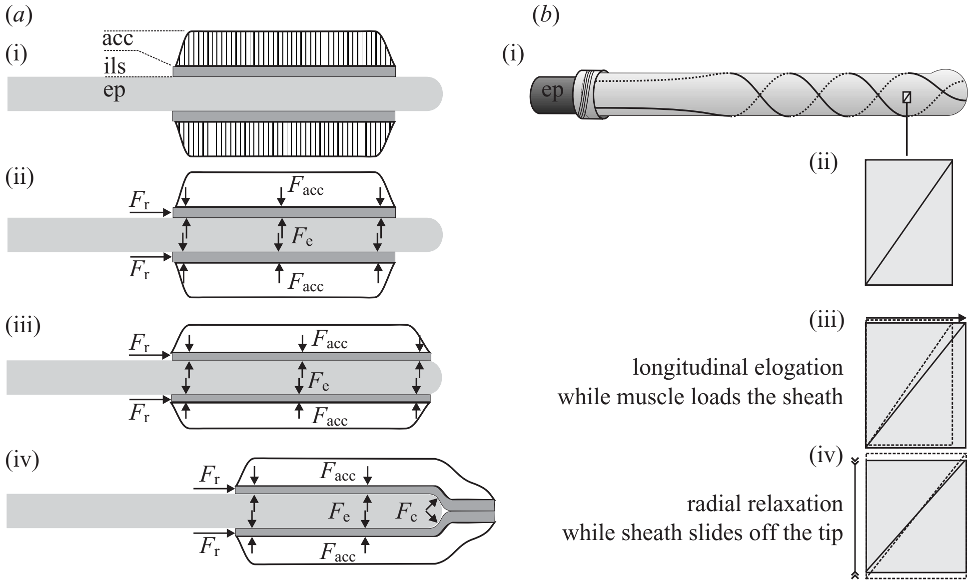

Figure 7. Schematic illustration of the loading of the intralingual sheaths by the accelerator muscle and the elastic release mechanism of the intralingual sheaths around the tip of the entoglossal process. (*a*)(i),(ii) The intralingual sheaths (ils) are loaded by compression between the activated accelerator muscle (acc, exerting force F_{acc}) and the entoglossal process (ep, exerting force F_{e}) and shear stresses from the accelerator muscle on the sheaths. Only the region of the sheaths that is loaded by the accelerator muscle is drawn. (iii) Radial thinning results in elongation of the muscle. The proximal margin of the muscle is prevented from backward motion by the maximally folded retractor complex, which pushes forward with force F_{r}. (iv) When the entoglossal tip is reached, projection is triggered and the 'loaded' accelerator muscle and sheaths start to move over the tip and elastic energy is released by the radial reduction of the sheaths. At the tip, the entoglossal process generates a forwardly directed force on the sheaths and the accelerator muscle that is transferred to both the tongue pad and the retractor complex through the central intralingual sheaths. (*b*) The mechanism of loading and release of elastic energy. A collagen fibre of an infinitesimal element in an intralingual sheath (i,ii; resting position) is stretched during the loading phase (iii). The circumferential length of the sheath is constant (because of the constant radius of the entoglossal process). Sheath elongation reorients, elongates and hence stresses the collagen fibres. The fibre stress has a longitudinal component along the entoglossal process and a circumferential component around the entoglossal process. (iv) At the tip, the fibre recoils owing to the decrease of the entoglossal and hence sheath radius. Thus, work is generated by the contracting collagen fibres that exert a stress on the entoglossal tip. Beyond the tip, the collagen fibres are relaxed.

observed lengthening of the accelerator muscle of *ca.* 33%, the recorded peak velocity of $5\ \mathrm{m\ s^{-1}}$ and an assumed maximum muscle stress of 200 kPa (Woledge *et al.* 1985). In order to elongate, the muscle acts like a hydrostat, in a similar way to a squid extending its tentacular stalks (Kier & Van Leeuwen 1997), but at a lower average longitudinal strain rate of *ca.* $0.33/(0.2\ \mathrm{s}) = 1.65\ \mathrm{s^{-1}}$. A simple mathematical simulation of the mechanism reveals that the work done in radial compression is negligible compared with the work done in muscular elongation: compression is *ca.* 2% of the longitudinal elongation. Hence, the muscle loads the sheaths elastically primarily by shear and by stretching the interconnections of the trabeculae with the peripheral intralingual sheaths. The normal and shear stresses exerted by the active muscle elongate the intralingual sheaths and load the internal helical collagen lattice. This loading pattern is consistent with the relatively high fluid content of the matrix (compared with tendons) and with the observed high local glycoprotein contents (concluded from a PAS positive reaction) of the peripheral sheaths.

(**b**) ***Elastic storage capacity of the generated work***

Energy generated by muscular stress is stored in the deformed intralingual sheaths and their matrix of collagen fibres. Despite the stiff collagen fibres, the intralingual sheaths allow sufficient deformation because the fibre angle with the longitudinal axis is *ca.* 55° in the internal epimysium and peripheral sheaths. As the cylinders elongate under external radial compressive and shear loads, the fibre angle must drop and fibre strain must rise. Effective loading of the sheaths requires force transfer via collagen trabeculae and shear and radial compression between neighbouring sheets, thereby elongating the most peripheral sheaths probably slightly more than the more central sheaths (figure 7*b*). Any possible shear forces between the innermost sheath and the tongue skeleton are reduced by the smooth and (presumed) lubricated entoglossal perichondrium. The portion of the central sheaths that posteriorly exceeds the posterior margin of the accelerator muscle, and therefore cannot be strained by it, contains longitudinally arranged collagen fibres (figure 4*b*(ii)), which is consistent with its force-transmitting function. In the anterior portion, which is covered by the accelerator muscle, the fibres are arranged in a helical fashion (figure 4*b*(iii)), which results in high extensibility and is consistent with its energy-storing function.

Without a means of obtaining the mechanical properties of the sheaths *in vivo*, their capacity to store energy is estimated as follows: based on the wet weight of the sheaths of a specimen of *C. melleri* (560 mg) and the required energy storage (80% of 72 mJ: 57.6 mJ), the energy stored in the sheaths is *ca.* $0.1\ \mathrm{mJ\ mm^{-3}}$. This value is approximately one-third of the value for sheep plantaris tendon under maximum physiological stress (Ker 1999) and five times the energy density of a maximally loaded human heel pad (Ker 1999). The tendon has a higher collagen-fibre density than the sheaths, and the heel pad has a lower fibre density (owing to the high fat content), which is in qualitative agreement with the present findings.

(c) *The quick-release mechanism*

The delayed release mechanism, proposed by Wainwright & Bennett (1992*b*), is consistent with the recorded forward elongation of the accelerator muscle prior to projection (figures 5*c* and 7*a*(ii,iii)) and the thickened tip of the entoglossal process, consisting of deformable connective tissue (see also Herrel *et al.* 2001*a*). This tip may initially function as a passive block, preventing any movement or downward orientation of the head resulting from releasing the tongue, and thus allowing the accelerator muscle to generate considerable pressures until the block is finally overcome when the anterior portion of the accelerator muscle and the loaded sheaths slide over and compress the entoglossal tip (figure 7*a*(iv)). The sudden decrease in internal diameter reduces the strain in the muscle and the sheath fibres (figure 7*a*(iv),*b*(iv)), and a quick release of the locally stored elastic energy follows. The distal reduction in muscle-fibre stress lowers the local pressure, generating a longitudinal negative pressure gradient towards the tongue tip, analogous to that found in the stalk of the tentacles in squid (Van Leeuwen & Kier 1997). According to our sliding-spring theory, the tongue accelerates forward, continuing the process of energy release, until the strained portion of the sheaths has slipped completely off the entoglossal tip. The locally distributed normal stress of the sheaths on the entoglossal tip results in a projecting force component. This force is distributed through the stiffened loaded intralingual sheaths along both the accelerator muscle and the retractor muscle, accelerating almost simultaneously the accelerator and retractor parts of the tongue. The release of the tongue starts only after the accelerator muscle has actively elongated by *ca.* 33% while storing elastic energy. The quick-release mechanism requires the peak acceleration to be above a minimum acceleration threshold, which was indeed observed. It also explains the observations of ourselves and Herrel *et al.* (2001*b*) that chameleons back off when prey is at a short distance, to ensure successful capture.

The proposed mechanism of tongue projection provides a coherent mechanistic explanation for the available previously published experimental data. The proposed mechanism encompasses interpretations of previous reports (Zoond 1933; Altevogt & Altevogt 1954; Bell 1990; Wainwright *et al.* 1991; Wainwright & Bennett 1992*a*,*b*; Van Leeuwen 1997). Conversely, we oppose the notion that the main projection power is generated directly by the accelerator muscle. Instead muscle power is slowly stored (over 200 ms) in the sheaths and later quickly released (in *ca.* 20 ms). This also explains the 10-fold drop in power that was recorded in *in situ* stimulation experiments that might have damaged (Zoond 1933) or even removed (Wainwright & Bennett 1992*b*) the intralingual sheaths.

The geniohyoid muscle (or mandibulohyoid muscle) inserts on the tongue skeleton and is essential for the normal projection of the tongue (Wainwright & Bennett 1992*a*; Meyers & Nishikawa 2000). It generates work during tongue protrusion and projection: *ca.* 10% of the peak power for projection and *ca.* 15% of the work throughout the projection process originates from this muscle. However, the extra momentum added to the tongue by the hyobranchium is low. With 15% of the kinetic energy originating from the hyobranchium, we see that $1/2\, m_{\mathrm{tongue}}(v^*_{\mathrm{max}})^2 = 1/2 \times 0.85\, m_{\mathrm{tongue}}(v_{\mathrm{max}})^2$, if $1/2\, m_{\mathrm{tongue}}(v^*_{\mathrm{max}})^2$ is the kinetic energy without the added energy from the hyobranchium and $1/2\, m_{\mathrm{tongue}}(v_{\mathrm{max}})^2$ is the kinetic energy of a normal shot (m_{tongue} is tongue mass, v_{max} is peak tongue velocity under normal conditions and v^*_{max} is the peak velocity if the entoglossal process transmitted zero energy). Thus, the momentum added to the tongue by the hyobranchium is $m_{\mathrm{tongue}}(v_{\mathrm{max}} - v^*_{\mathrm{max}}) = m_{\mathrm{tongue}}(v_{\mathrm{max}} - 0.85^{1/2} v_{\mathrm{max}}) = 0.078 v_{\mathrm{max}}\, m_{\mathrm{tongue}}$, only a small fraction of the total momentum. Denervation of the geniohyoid muscle considerably reduces tongue projection (Meyers & Nishikawa 2000). This loss in power is not caused by the geniohyoid muscle no longer contributing power. Instead a denervated and inactive geniohyoid muscle can no longer provide the forwardly directed posterior force that needs to be applied to the entoglossal process to stabilize the tongue skeleton when it is hit by the rebound of the tongue pad. The rebound causes the soft tongue parts to do work on the entoglossal process and this is no longer available for tongue-pad projection. Thus, the process absorbs a considerable part of the available projection energy released by the sheaths and consequently reduces projection performance. We hope that the present results help to settle the controversies in the literature about the role of the hyoid apparatus in tongue projection.

Elastic-energy storage and release often occur along reversible pathways of (forceful) elongation and shortening. For instance, in a jumping locust, contracting muscles apply a tensile load to an apodeme. The strain energy is later released as the apodeme shortens, extending the leg and accelerating the body (Alexander 1983). In the chameleon tongue, the intralingual sheaths are longitudinally strained prior to projection, while the inner diameters of the sheaths are kept almost constant (figure 7*a*(ii,iii),*b*(ii,iii)). The tensile-strain energy is stored in the helical collagen fibres of the sheaths, until the loaded portion of the sheaths starts to slide over the tip of the entoglossal process. This allows the inner radius of the sheaths to decrease (figure 7*a*(iii,iv)), releasing the tensile energy and generating work until the loaded portion of the accelerator muscle and the underlying sheaths have passed the entoglossal tip. This process ensures a continuing (fairly constant) force to accelerate the tongue with increasing power, unlike the longitudinal release in tendons, which generates initially high, but exponentially decreasing, forces. Applied to the soft tissue of the tongue (instead of stiff skeletal elements), such a reversible longitudinal release mechanism would cause higher internal deformations of the tongue, which, in turn, would dissipate a relatively large portion of the stored energy, whereas the relatively constant force in the chameleon tongue reduces the internal deformation of the soft body. On a molecular level, however, both mechanisms are reversible, based on the elongation and shortening of elastic (collagen) molecules.

The family Plethodontidae (a group of lungless salamanders) independently evolved tongue projections that are similar in performance to those found in chameleons (Lombard & Wake 1977). In *Hydromantes supramontis*, the forked hyobranchial skeleton is projected out of the mouth, whereas the protractor muscles that, at rest, envelop the skeleton remain inside the mouth (Deban *et al.* 1997). Quite interestingly, a substantial connective-tissue layer is also present between the muscles and the tongue skeleton, which could have a similar role to the connective-tissue sheaths in the chameleon. This analysis underpins the suggestion of Van Leeuwen *et al.* (2000) that the extreme tongue-projection performance in the genus *Hydromantes* requires an elastic mechanism.

In conclusion, we have strong experimental and morphological evidence that tongue projection in the chameleon involves elastic-energy storage and release, and that the intralingual sheaths play a major role in this mechanism. The unique tongue mechanism deviates from the conventional catapult design in its multilayered tubular springs with helically arranged fibres and associated accelerator muscle, the forward motion during loading, initiation of projection by extension of the anterior springs beyond the entoglossal tip, and the sequential energy release along the springs by sliding and radial thinning. The salient features of the proposed mechanism agree with the available previous experimental observations and with the structural components present in the tongue. The next challenge is to construct a biomechanical model of the system that predicts the tongue projection quantitatively.

The authors thank Peter Snelderwaard and Merijn Bakker for their skilled technical support, Gideon Bevelander for the microscopic data on fibre angles, Dr Herman Berkhoudt for the photography, and Dr William Kier, Dr Mees Muller, Dr Steve Deban, Dr Ulrike Müller and Dr Leonard Rozendaal for their helpful and stimulating comments on draft versions of this paper. This research was supported by the Earth and Life Sciences Foundation (ALW), subsidized by the Netherlands Organization for Scientific Research (NWO).

REFERENCES

Alexander, R. McN. 1983 *Animal mechanics*, 2nd edn. Oxford: Blackwell Scientific.

Altevogt, R. & Altevogt, R. 1954 Studien zur Kinematik der Chamäleonzunge. *Z. Vergl. Physiol.* **36**, 66–77.

Askew, G. N. & Marsh, R. L. 2001 The mechanical power output of the pectoralis muscle of blue-breasted quail (*Coturnix chinensis*): the *in vivo* length cycle and its implications for muscle performance. *J. Exp. Biol.* **204**, 3587–3600.

Bell, D. A. 1989 Functional anatomy of the chameleon tongue. *Zool. Jahrbücher Anat.* **119**, 313–336.

Bell, D. A. 1990 Kinematics of prey capture in the chameleon. *Zool. Jahrbücher Physiol.* **94**, 247–260.

Deban, S. M., Wake, D. B. & Roth, G. 1997 Salamander with a ballistic tongue. *Nature* **389**, 27–28.

Duvernoy, G. L. 1836 Sur les movement de la langue du caméléon. *Compt. Rend. hebd. Séanc. Acad. Sci. Paris* **2**, 349–351.

Gans, C. 1967 The chameleon. *Nat. Hist.* **76**, 52–59.

Gnanamuthu, C. P. 1930 The anatomy and mechanism of the chameleon tongue of *Chamaeleo carcaratus* (Merrem). *Proc. Zool. Soc. Lond.* **31**, 467–486.

Gnanamuthu, C. P. 1937 Comparative study of the hyoid and tongue of some typical genera of reptiles. *Proc. Zool. Soc. Lond.* B **107**, 1–63.

Harkness, L. 1977 Chameleons use accommodation cues to judge distance. *Nature* **267**, 346–351.

Herrel, A., Meyers, J. J., Aerts, P. & Nishikawa, K. C. 2000 The mechanism of prey prehension in chameleons. *J. Exp. Biol.* **203**, 3255–3263.

Herrel, A., Meyers, J. J., Nishikawa, K. C. & De Vree, F. 2001*a* Morphology and histochemistry of the hyolingual apparatus in chameleons. *J. Morphol.* **249**, 154–170.

Herrel, A., Meyers, J. J., Aerts, P. & Nishikawa, K. C. 2001*b* Functional implications of supercontracting muscle in the chameleon tongue retractors. *J. Exp. Biol.* **204**, 3621–3627.

Ker, R. F. 1999 The design of soft collagenous load-bearing tissues. *J. Exp. Biol.* **202**, 3315–3324.

Kier, W. M. & Van Leeuwen, J. L. 1997 A kinematic analysis of tentacle extension in the squid *Loligo pealei*. *J. Exp. Biol.* **200**, 41–53.

Lombard, R. E. & Wake, D. B. 1977 Tongue evolution in lungless salamanders, Family Plethodontidae. II. Function and evolutionary diversity. *J. Morphol.* **153**, 39–80.

Lutz, G. J. & Rome, L. C. 1994 Built for jumping: the design of the frog muscular system. *Science* **263**, 370–372.

Meyers, J. J. & Nishikawa, K. C. 2000 Comparative study of tongue protrusion in three iguanian lizards, *Sceloporus undulatus*, *Pseudotrapelus sinaitus* and *Chamelao jacsonii*. *J. Exp. Biol.* **203**, 2833–2849.

Ott, M. & Schaeffel, F. A. 1995 Negatively powered lens in the chameleon. *Nature* **373**, 692–694.

Rice, M. G. 1973 Supercontracting striated muscle in a vertebrate. *Nature* **243**, 238–240.

Snelderwaard, P. Ch., De Groot, J. H. & Deban, S. M. 2002 Digital video combined with conventional radiography creates an excellent high-speed X-ray video system. *J. Biomech.* **35**, 1007–1009.

Van Leeuwen, J. L. 1997 Why the chameleon has spiral-shaped muscle fibres in its tongue. *Phil. Trans. R. Soc. Lond.* B **352**, 573–589. (DOI 10.1098/rstb.1997.0039.)

Van Leeuwen, J. L. & Kier, W. M. 1997 Functional design of tentacles in squid: linking sarcomere ultrastructure to gross morphological design. *Phil. Trans. R. Soc. Lond.* B **352**, 551–571. (DOI 10.1098/rstb.1997.0038.)

Van Leeuwen, J. L., de Groot, J. H. & Kier, W. M. 2000 Evolutionary mechanics of protrusible tentacles and tongues. *Neth. J. Zool.* **50**, 113–139.

Wainwright, P. C. & Bennett, A. F. 1992*a* The mechanism of tongue projection in chameleons. I. Electromyographic tests of functional hypotheses. *J. Exp. Biol.* **168**, 1–21.

Wainwright, P. C. & Bennett, A. F. 1992*b* The mechanism of tongue projection in chameleons. II. Role of shape change in a muscular hydrostat. *J. Exp. Biol.* **168**, 23–40.

Wainwright, P. C., Kraklau, D. M. & Bennett, A. F. 1991 Kinematics of the tongue projection in *Chamaeleo oustaleti*. *J. Exp. Biol.* **159**, 109–133.

Woledge, R. C., Curtis, N. A. & Homsher, E. 1985 *Energetic aspects of muscle contraction*. Monographs of the Physiological Society no. 41. London: Academic.

Zoond, A. 1933 The mechanism of projection of the chameleon's tongue. *J. Exp. Biol.* **10**, 174–185.

As this paper exceeds the maximum length normally permitted, the authors have agreed to contribute to production costs.

Visit www.journals.royalsoc.ac.uk and navigate to this article through *Proceedings*: Biological Sciences to see the accompanying electronic appendix.